ELECTRONIC STIMULATION OF INTERSTITIAL DEFECT REACTIONS IN IRRADIATED P-TYPE SILICON

L.F. Makarenko,[a] S.B. Lastovski,[b] M. Moll,[c] I. Pintilie,[d]

[a] *Belarusian State University, Minsk, Belarus,*
[b] *Scientific-Practical Materials Research Centre of NAS of Belarus, Minsk, Belarus*
[c] *CERN, Geneva, Switzerland,*
[d] *NIMP, Bucharest, Romania,*

Recombination enhancement of defect reactions in semiconductors

Recombination enhancement of defect reactions is typically observed in compound semiconductors [1, 2].

In silicon, the recombination enhancement of migration was found to be characteristic for many single interstitial atoms formed as result of irradiation. These are silicon self-interstitial (Si_i) [3], aluminum interstitial (Al_i) [4], boron interstitial (B_i) [5] and carbon interstitial (C_i) [6].

Vacancy related radiation defects in silicon are also sensitive to electronic excitation. Those are for example injection-enhanced reordering of vacancies in Si solar cells observed at low temperatures [7] and forward current enhanced (FCE) annealing of the donor-vacancy complex (E-center) [8].

In this talk we present our recent results on FCE annealing studies of interstitial boron-interstitial oxygen (BiOi) complex and interstitial carbon.

1. L. Kimerling, Recombination enhanced defect reactions. Solid-State Electronics, **21**, 1391 (1978).
2. D. V. Lang, Recombination-enhanced reactions in semiconductors. Annual review of materials science, 12(1), 377-398 (1982).
3. G. D. Watkins, Radiation damage in semiconductors (Dunod, Paris, 1965). p. 97.
4. J. R. Troxell, A. P. Chatterjee, G. D. Watkins, and L. C. Kimerling, Phys. Rev. B, **19**, 5336 (1979).
5. J. R. Troxell, G. D. Watkins Phys. Rev. B. **22**, 921 (1980).
6. A. R. Frederickson, A. S. Karakashian, P. J. Drevinsky, and C. E. Caefer, J. Appl. Phys., **65**, 3272 (1989).
7. B. L. Gregory, J. Appl. Phys. **36**, 3765 (1965):
8. C. E. Barnes, and G. A. Samara, Appl. Phys. Lett. 48, 934 (1986):

Background impurities in epitaxial structures

Oxygen and carbon can be appeared
a) during epitaxial growth;
b) during technological processing of structures.

Typical background impurity distribution was obtained earlier by SIMS method.

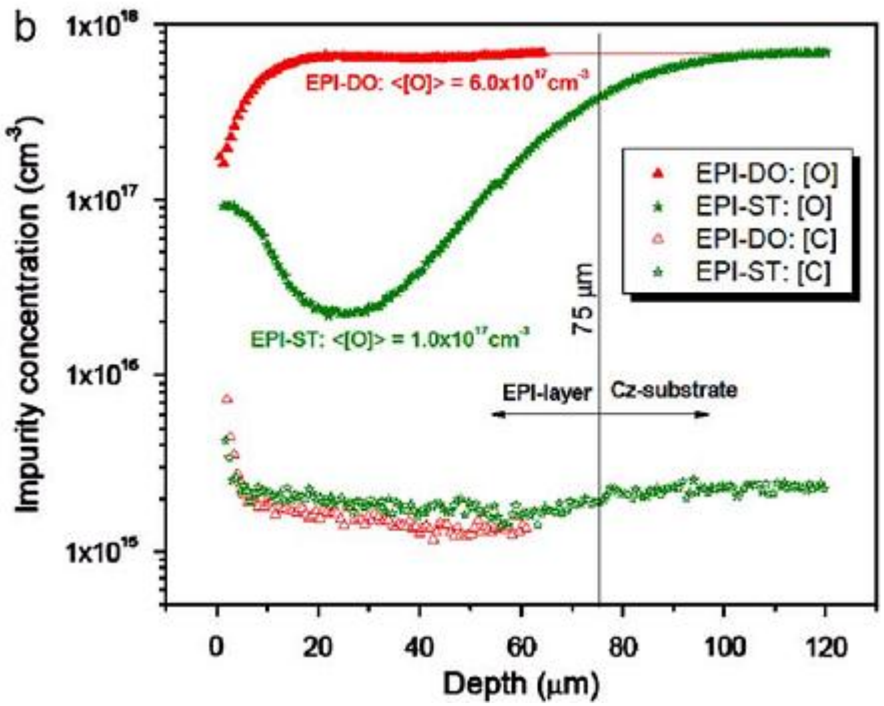

Fig. 1. Depth profiles of oxygen and carbon concentrations measured with SIMS in EPI-ST and EPI-DO diodes;

Ioana Pintilie, Gunnar Lindstroem, Alexandra Junkes,Eckhart Fretwurst, Nuclear Instruments and Methods in Physics Research A 611 (2009) 52–68

Evaluation of oxygen content

Oxygen content can be also determined by electrical measurements from the kinetics of interstitial carbon reaction:

$$C_i + O_i \rightarrow C_iO_i$$

(see Makarenko, L. F., Moll, M., Korshunov, F. P., & Lastovski, S. B. (2007). Reactions of interstitial carbon with impurities in silicon particle detectors. Journal of applied physics, 101(11), 113537.)

Or from the kinetics of divacancy annealing:

$$V_2 + O_i \rightarrow V_2O$$

(see Mikelsen, M., Monakhov, E. V., Alfieri, G., Avset, B. S., & Svensson, B. G. (2005). Kinetics of divacancy annealing and divacancy-oxygen formation in oxygen-enriched high-purity silicon. Physical Review B, 72(19), 195207)

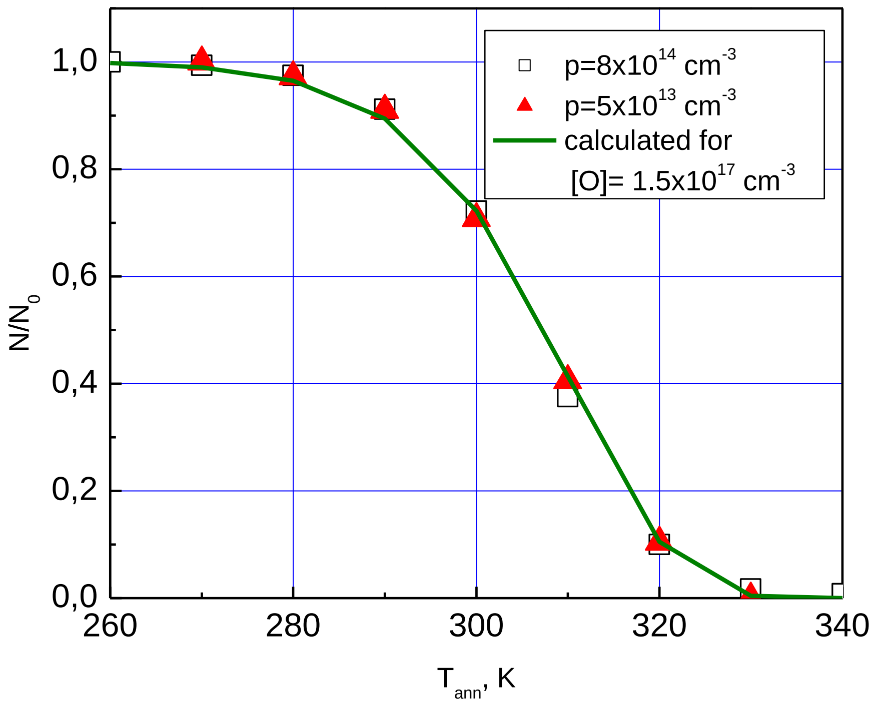

Fig.2. Isochronal annealing of interstitial carbon in epitaxial n^+-p structures made in Minsk in 2006 (squares) and in 2013 (trianges).

One can see the good repeatability of technological regimes.

Evaluation of carbon content

a) When carbon and oxygen concentration are comparable then carbon content can be evaluated by the ratio between concentrations of C_iO_i and C_iC_s complexes.

b) When oxygen has much higher concentration than carbon, one can use the ratio between concentrations of C_iO_i and B_iO_i complexes:

$$\eta = \frac{[B_iO_i]}{[C_iO_i]}$$

However this method is not easy to get adequate results. There are some features which should be taken into account. Let’s consider factors which influence on the ratio η.

Effect of irradiation type and post-irradiation treatment on η

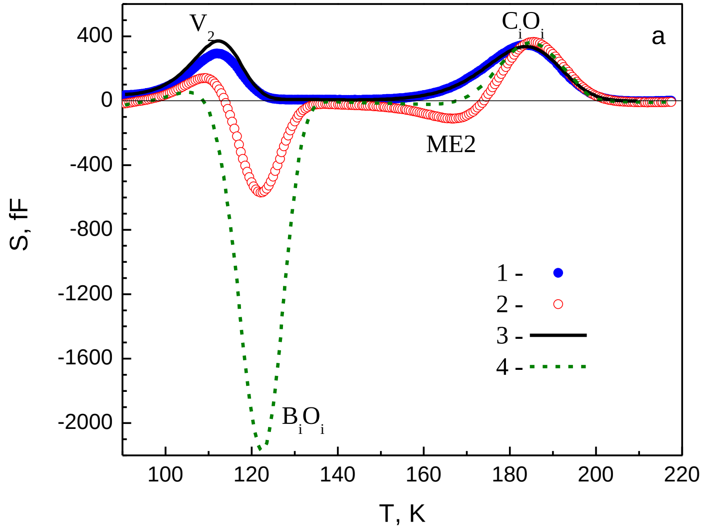

Fig.3. DLTS and MC-DLTS spectra for n^+-p structures made of epitaxial silicon irradiated with Pu-239 alpha-particles. The irradiation time was 16 hours at temperature not higher than 290 K. All the spectra were measured after annealing at 100 °C for 30 minutes. The annealing was performed either immediately after irradiation (lines) or after irradiation followed by a forward current injection performed at 78 K (circles).

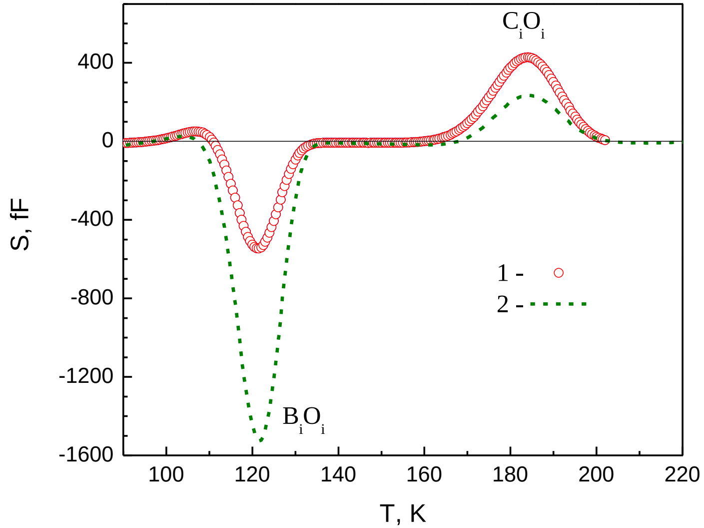

Fig.4. MC-DLTS spectra for n^+-p structures made of epitaxial silicon irradiated with Pu-239 alpha-particles (curve 1) and electrons with E=5.5 MeV (curve 2). All the spectra were measured after annealing at 100 °C for 30 minutes. The annealing was performed immediately after irradiation. Post-irradiation injection doesn't change the peak heights after electron irradiation.

Comparison of diodes with different base doping

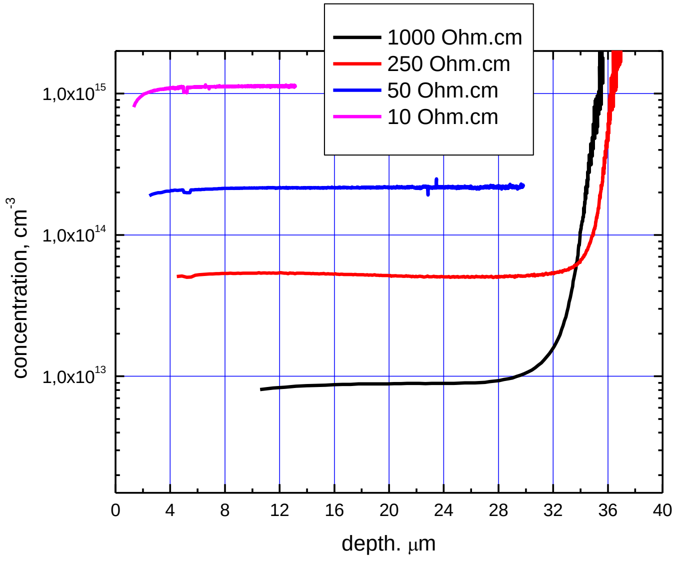

Fig.5. Hole concentration in epitaxial structures as determined from C-V measurements. All the structures were produced with same technological procedure.

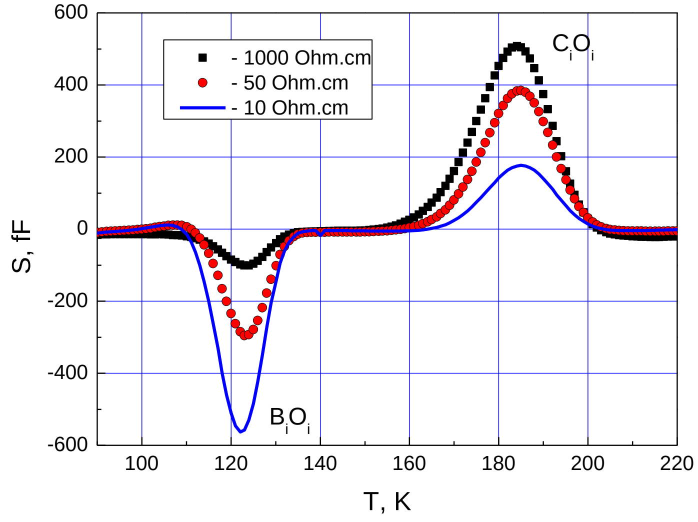

Fig.6. MC-DLTS spectra for the diodes from the previous figure.

If we suggest that the 10 Ohm.cm structures have carbon concentration about 10^{15} cm^{-3}, then for the 1000 Ohm.cm structures we obtain carbon concentration about 10^{14} cm^{-3}. That is there exists a correlation between boron and carbon content in epitaxial diodes. It can also be related to the depth distribution of carbon.

Thermal annealing of B_iO_i

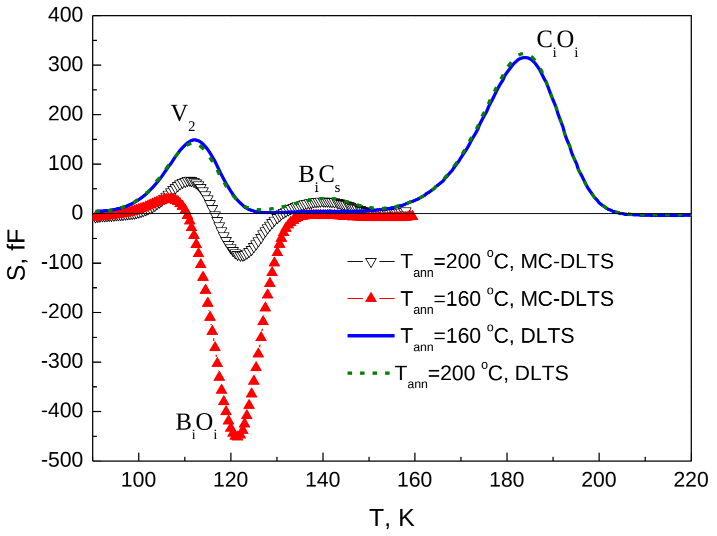

Fig.7. Evolution of DLTS (lines) and MC-DLTS (triangles) spectra during disappearance of B_iO_i (peak E1) in Si n^+-p structures irradiated with electrons (E=3.5 MeV). The spectra were measured after 20 minutes annealing at 160 °C (solid lines and filled triangles) and 200 °C (dash lines and empty triangles)

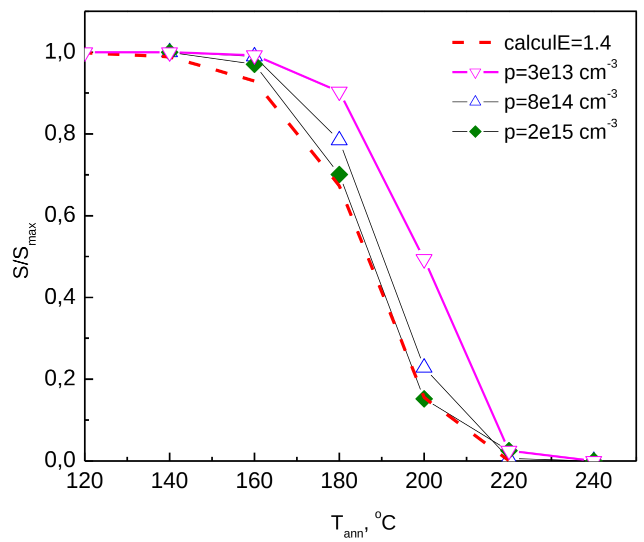

Fig.8. Isochronal annealing of BiOi complex in Si diodes with different base doping. Annealing settings were: ΔT = 20 K, Δt = 20 min.

There are no recovery of hole concentration after B_iO_i disappearance. Activation energy of B_iO_i annealing was determined as close to 1.4 eV.

It was suggested that the thermal annealing characteristics can be explained by two main reactions:

$$B_iO_i \leftrightarrow B_i + O_i$$

$$B_i + B_s \rightarrow B_iB_s$$

The higher is oxygen content the faster is the B_iO_i annealing rate.
The higher is oxygen content the slower is the B_iO_i annealing rate.

The B_iB_s complex is electrically neutral.
But there is no information on its stability.

Recombination enhancement of interstitial aluminium, boron and carbon migration in Si

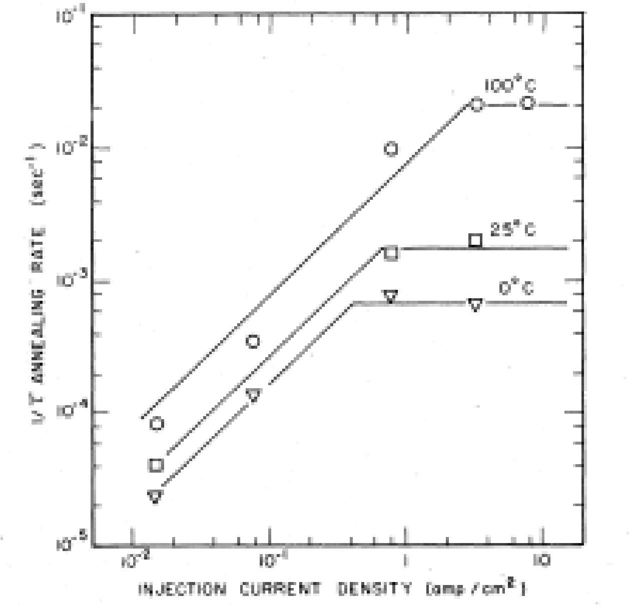

FIG. 4. *H*3 defect recovery rate as a function of injection current density at 0, 25, and 100 °C.

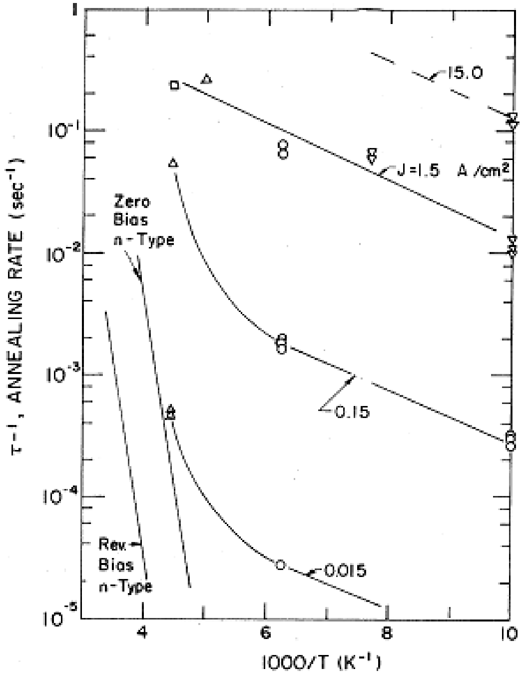

FIG. 4. Annealing kinetics for the growth of the *E*(0.23) level in *p*-type material under minority-carrier injection conditions. (O, □, ∇, Δ refer to data taken on different samples.) Points connected by the curves were measured for the injection current density indicated. Shown for comparison are the zero- and reverse-bias results in *n*-type material.

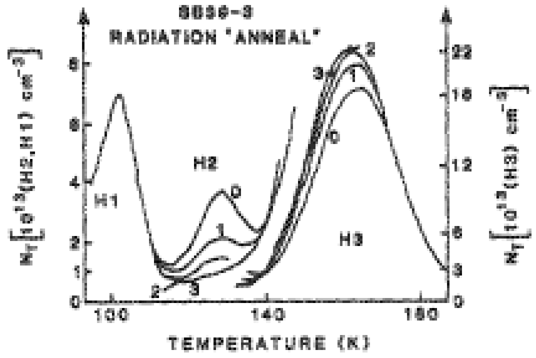

FIG. 2. DLTS data showing radiation-induced annealing of H3 and accompanying growth of H3 in electron-irradiated CZ silicon. Curve 0 is shortly after 1-MeV irradiation. Curves 1, 2, and 3 are after 1×10^{14}, 2×10^{14}, and 1.2×10^{15} LE electrons cm^{-2}, respectively. Peaks H1 and H2 were measured at a more sensitive lock-in detector setting. Amplitude at a peak indicates the trap density.

Troxell, J. R., & Watkins, G. D. (1980). Interstitial boron in silicon: A negative-U system. *Physical Review B*, **22**(2), 921.

Troxell, J. R., Chatterjee, A. P., Watkins, G. D., & Kimerling, L. C. (1979). *Physical Review B*, **19**(10), 5336.

Frederickson, A. R., Karakashian, A. S., Drevinsky, P. J., & Caefer, C. E. (1989). *Journal of Applied Physics*, **65**(8), 3272-3274.

Effect of forward current on the B_iO_i annealing

For these studies we used p+-n diodes made from 10 and 50 Ohm·cm silicon. Forward currents were in the range 10-30 A/cm^2.

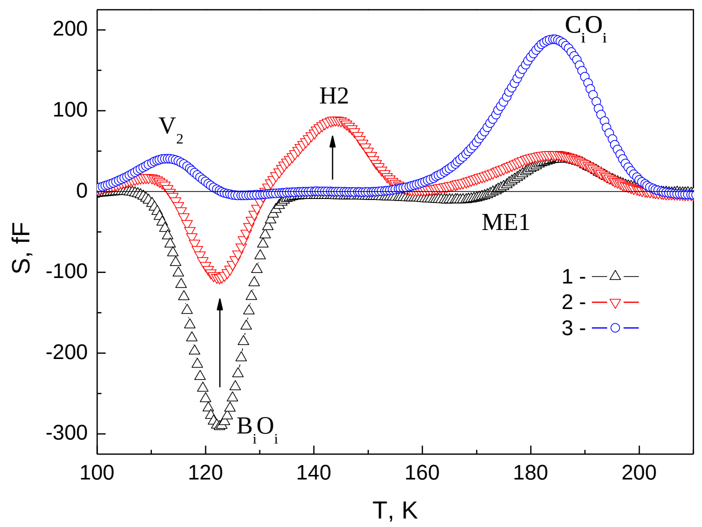

Fig.9. MC-DLTS spectra obtained on samples irradiated for 100 minutes. The curve 1 represents MC-DLTS spectra obtained after irradiation and preliminary annealing for 30 minutes at 120 °C. The curve 2 was recorded after 20 minutes of FCE annealing at 280 K and the curve 3 after the complete transformation of C_i (H2) into C_iO_i (H3) (curves 3′).

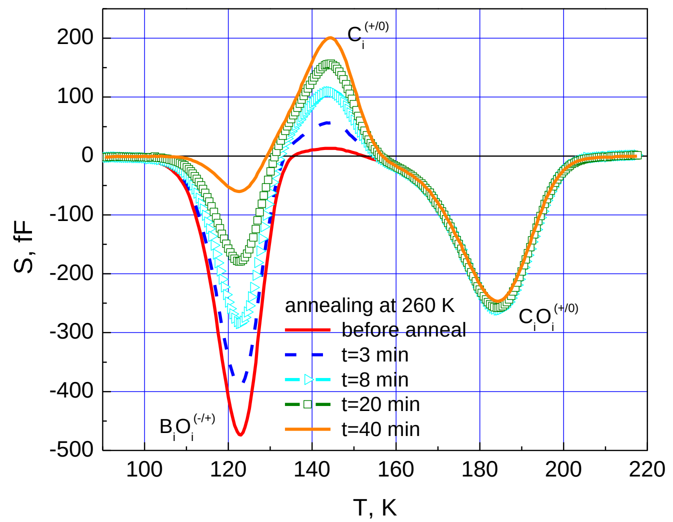

Fig.10. The difference between MC-DLTS spectra registered after FCE annealing and registered after stabilization annealing at 70 °C.

There is a correlation:

The increase of carbon related DLTS signal (C_i+C_iO_i) is twice less than decrease of B_iO_i DLTS signal.

We interpret this correlation as related to negative-U properties of B_iO_i complex.

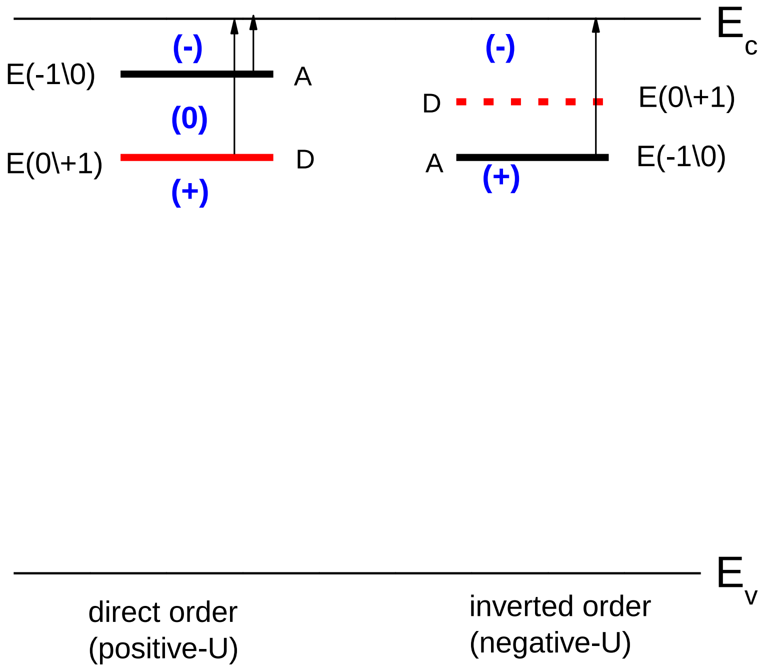

This means that DLTS signal of B_iO_i corresponds to the emission of two electrons simultaneously and the E_c-0.23 eV level seen in the DLTS spectra corresponds to acceptor level of this complex.

It is well known that Si self-interstitial and interstitial boron are negative-U centers.
Possibly, interstitial aluminum also is also a negative-U center.
But interstitial carbon is known as a positive-U center.

Effect of forward current on the C_i annealing

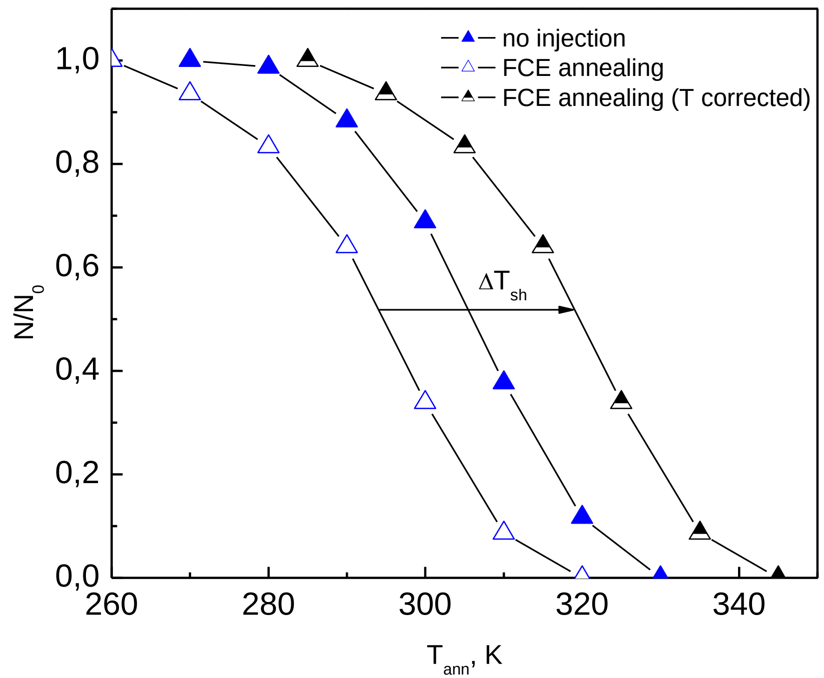

Fig. 13. Isochronal annealing behavior of C_i in Si diodes under thermal equilibrium (filled symbols) and under forward current injection (empty symbols) conditions, in steps of .10 K, with annealing time 15 minutes. The temperature shift (ΔT_{sh}) takes into account the diode self-heating.

Fluence and current dependence of the FCE annealing

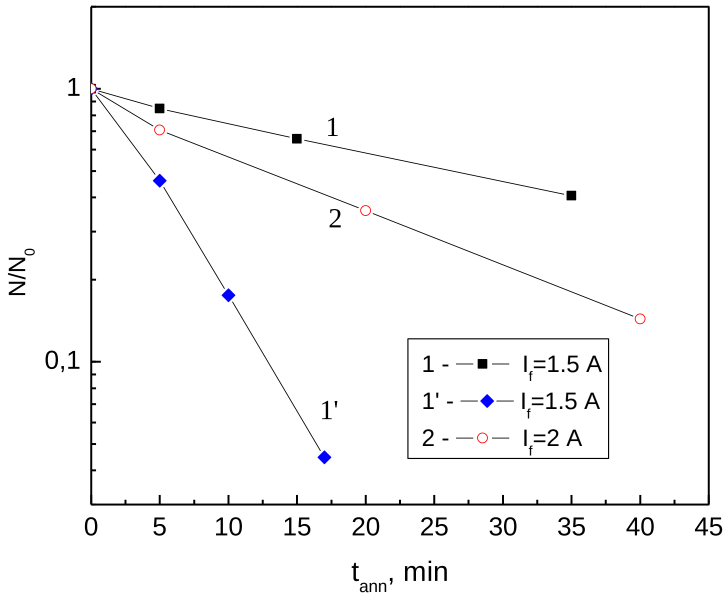

Fig.11. Kinetics of B_iO_i disappearance during the isothermal FCE annealing at 300 K (t_{ann}) for different forward current densities (J_f) and for different irradiation times (t_{irr}). The curve 1 was obtained after irradiation during 900 min. and irradiation time for the curve 1′ was 10 times less.

It can be explained as the result of different minority carrier densities under forward current injection and due to self-heating.

Temperature dependence of the FCE annealing

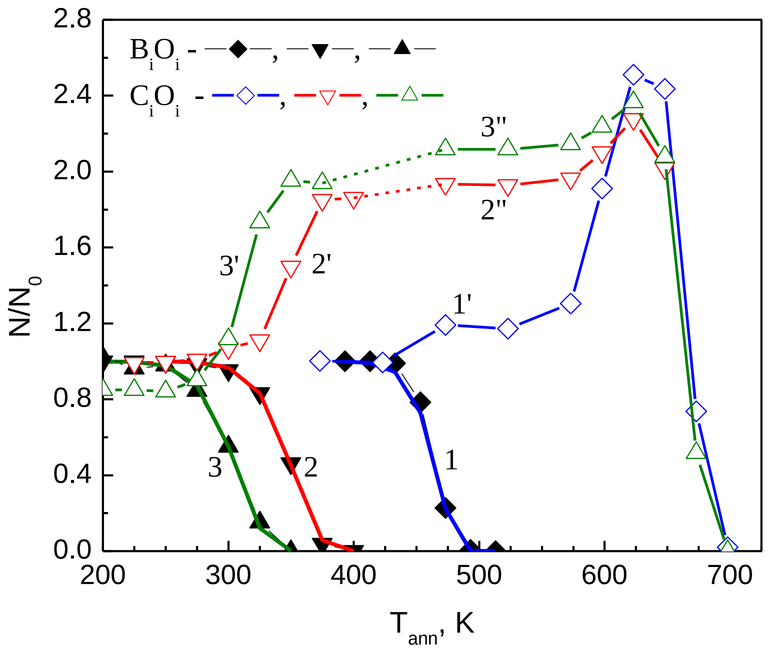

Fig.12. Isochronal annealing behavior of B_iO_i (filled symbols) and C_iO_i (empty symbols) complexes, in steps of 25 K, for samples irradiated for 900 minutes. Results of the 30 minutes thermal annealing ($J_f=0$ *A/cm*^{2}) at each temperature are given by the blue curves 1, 1′ and 2″, 3″. The FCE annealing was performed between 200 K and 400 K for 10 minutes at each temperature and for two different forward currents: $J_f=24$ *A/cm*^{2} (curves 2, 2′) and $J_f=32$ *A/cm*^{2} (curves 3, 3′). The fitting curves for the B_iO_i annealing are given as thick solid lines.

The resulting activation energies are in the range of E_a=0.4-0.6 eV for current densities between 15 and 30 A/cm^2.

These results demonstrate that the annealing of the B_iO_i complex is accompanied by the appearance of interstitial carbon. In our opinion, such a process can occur considering three consecutive defect reactions: (i) the recombination enhanced dissociation of B_iO_i and appearance of B_i, (ii) an inverse Watkins replacement reaction for interstitial boron

$$B_i + Si_s + M \to B_s + Si_i + M^*$$

and (iii) a direct Watkins replacement reaction for substitutional carbon

$$C_s + Si_i \to C_i.$$

As M in reaction (1) we denote a possible mediator or a component of an intermediate complex, and finally:

$$C_i + O_i \to C_iO_i$$

When concentration of C_iO_i is quite large it can effectively capture Si self-interstitials (see L.I. Murin et al. Solid State Phenomena Vols. 205-206 (2014) pp 218-223) and form C4-center.

Conclusions

Comparing introduction rates of boron and carbon related complexes we can, in principle, evaluate very low carbon content in Si n^+-p diodes even if oxygen concentration is quite high.

Using forward current injection at room temperature with densities in the range 15-30 A/cm^2 we can effectively eliminate the radiation induced boron-oxygen complex.

There is no enhancement of interstitial carbon annealing by forward current injection.